Performance of a Boron-Coated-Straw-Based HLNCC for International Safeguards Applications

Angela T. Simone, *Member, IEEE*, Stephen Croft, Robert D. McElroy, Jr., Liang Sun, *Member, IEEE*, Jeffrey L. Lacy, *Member, IEEE*, Athanasios Athanasiades, *Member, IEEE*, and Jason P. Hayward, *Member, IEEE*

IEEE Proof

***Abstract*—^{3}He gas has been used in various scientific and security applications for decades, but it is now in short supply. Alternatives to ^{3}He detectors are currently being integrated and tested in neutron coincidence counter designs, of a type which are widely used in nuclear safeguards for nuclear materials assay. A boron-coated-straw-based design, similar to the high-level neutron coincidence counter-II, was built by Proportional Technologies Inc., and has been tested by the Oak Ridge National Laboratory (ORNL) at both the JRC in Ispra and ORNL. Characterization measurements, along with nondestructive assays of various plutonium samples, have been conducted to determine the performance of this coincidence counter replacement in comparison with other similar counters. This paper presents results of these measurements.**

***Index Terms*—^{3}He alternatives, boron-coated straws (BCSs), coincidence counter, neutron detection, safeguards.**

I. Introduction

FOR decades, ^{3}He-filled proportional counters have been the gold standard for the detection of slow neutrons, offering high neutron efficiency and excellent discrimination against gamma rays. They are extensively used for the nondestructive assay of special nuclear materials (SNMs). However, due to the decreased supply and increased demand for the gas [1], [2], joint efforts have been made by the U.S. Department of Energy's National Nuclear Security Administration [3] and Euratom to find a viable replacement for neutron detection.

Scintillating ^{6}Li-glass-loaded glass fibers have been previously tested for homeland security applications [4], and efforts have moved to extend this technology to the safeguards field. They can achieve comparable sensitivity to ^{3}He tube assemblies [5]–[7], despite a significantly lower cross section of ^{6}Li compared with ^{3}He, because higher number densities can be used. The neutron die-away time can also be much shorter than standard ^{3}He tube designs since the ^{6}Li is more evenly distributed throughout the moderator. Gamma interactions in the scintillation fibers result in less light production and thus, signals of smaller amplitude. These designs must apply electronic pulse height discrimination to distinguish the particles. As the pulse rate increases, the dead time within the electronics increases and counts are lost. Also, as the volume of the detector increases to achieve a greater efficiency, the pulse differences between neutrons and gamma rays become more difficult to discern [8]. Pulse pileup becomes limiting in high-rate applications due to the necessary electronics and long luminescence lifetime [9].

Currently, designs implementing LiF/ZnS(Ag) scintillators are also under investigation [10]–[12], with emphasis on neutron multiplicity detector designs from PNNL [13]–[15], and Symetrica Ltd. and JRC [3], [16]. The Symetrica Ltd. design incorporates blade detectors surrounded by a moderating body, with a high efficiency and low die-away time. At the time of the measurement reported in this paper, only two of the four panels of the blades had been tested as an assembly. However, simulations of a fully populated system support the proposition that this design may be a viable alternative provided real time pulse discrimination will be commensurate with a short predelay compared to the die-away time [3].

The IAEA's development, with Hybrid Instruments Ltd., of the liquid scintillator-based neutron coincidence counter is proposed to be used for the active measurement of fast neutrons from low-enriched uranium fuel [3], [17], [18]. Algorithms to minimize crosstalk between scintillators, scatter-induced coincidences, and system dead time, in addition to pulse-shape discrimination, are necessary for this technique [18]–[20]. The University of Michigan coincidence counter design, based upon EJ-309 and stilbene plastic scintillation detectors, has been shown to distinguish time-correlated neutron events from random neutrons and gammas [21], [22] with the relevant electronics and data processing. They are also working on methods to account for fast-neutron scatter. Liquids have yet to be accepted in nuclear plants and

AQ:1 Manuscript received May 10, 2017; revised July 25, 2017; accepted August 7, 2017. This work was supported in part by the DOE/NNSA Office of Nonproliferation and Arms Control (NA-24) and in part by UT-Battelle, LLC, through the U.S. Department of Energy under Contract DE-AC05-00OR22725.

A. T. Simone and J. P. Hayward are with the University of Tennessee, Knoxville, TN 37996 USA, and also with the Oak Ridge National Laboratory, Oak Ridge, TN 37831 USA (e-mail: simoneat@ornl.gov).

S. Croft and R. D. McElroy, Jr., are with the Oak Ridge National Laboratory, Oak Ridge, TN 37831 USA.

L. Sun, J. L. Lacy, and A. Athanasiades are with Proportional Technologies, Inc., Houston, TX 77054 USA.

Color versions of one or more of the figures in this paper are available online at http://ieeexplore.ieee.org.

Digital Object Identifier 10.1109/TNS.2017.2742986

0018-9499 © 2017 IEEE. Personal use is permitted, but republication/redistribution requires IEEE permission.
See http://www.ieee.org/publications_standards/publications/rights/index.html for more information.

engineering due to the confines of ease in setup and use, in addition to stability requirements.

Alternatives exploiting boron have the advantage of the second highest cross section, 3835 b, compared to ^{3}He, with a cross section of 5333 b at 2200 m/s. The gamma-ray noise is low enough to be distinguished from charged particle pulses by setting a threshold value, permitting high gamma insensitivity. BF_3-filled proportional detectors meet the requirements specified for a drop-in replacement technology, yet the gas is toxic and heavily regulated by the Department of Transportation, and is therefore not ideal to be deployed in the field. When size is not a restriction, such as in portal monitors, efficiency can be achieved by using more BF_3 tubes with less fill pressure than the equivalent ^{3}He tube-based systems.

Current technologies implementing thin ^{10}B deposits on their surfaces offer no health risk, unlike BF_3 tubes, while utilizing the same physics for detection. The Precision Data Technology-designed parallel-plate boron proportional counters have been tested by the Los Alamos National Laboratory (LANL). At the time of the reported measurement, the large amount of moderating material in the system increased the neutron die-away time compared to the benchmark ^{3}He model [23]. An upgraded system is being built and tested to improve dead time and die-away time [24], [25]. A class of commercial General Electric Reuter-Stokes ^{10}B-lined proportional tubes have been built into a system, simulated, and then tested at PNNL [26], [27]. For the current system design, the resulting efficiency, neutron die-away time, detector dimensions, and necessary count duration for low statistical uncertainty have not met the declared standards for replacement [3], [27], yet this model may suffice for other international safeguards applications that are not limited to such constraints [28].

Two workshops have been held in recent years to bring together international experts and developers of these technologies. Both the ^{3}He alternatives for International Safeguards Workshops at LANL in 2013 and the JRC in Ispra in 2014 [3] brought together six plausible prototypes for benchmark tests and comparisons to three currently used ^{3}He coincidence counters: 1) the high-level neutron coincidence counter-II (HLNCC-II); 2) the Uranium Neutron Collar (UNCL); and 3) and the UNCL slab. These prototypes were built based upon: 1) LiF/ZnS(Ag) scintillators coupled to polyvinyl toluene wavelength shifters (Symetrica); 2) Stilbene scintillators (University of Michigan/Lawrence Livermore National Laboratory); 3) liquid scintillators model EJ-309 (International Atomic Energy Agency, IAEA); 4) parallel-plate boron proportional counters (Precision Data Technology); 5) boron-lined tubes (GE Reuter-Stokes); and 6) boron-coated straws [Proportional Technologies Inc., (PTI)].

This paper reports on the measurement results for a boron-coated-straw (BCS)-based HLNCC. The HLNCC-II is widely used by IAEA inspectors in many nuclear facilities for passive neutron coincidence counting of plutonium samples and gram to kilogram quantities of mixed oxide materials. More specifically, we report on measurements including the high-voltage (HV) characteristic, detector efficiency, neutron die-away time, and Pu mass assay. We also compare the results to the ^{3}He-based HLNCC-II and the other developing ^{3}He replacement technologies including systems based upon GE Reuter-Stokes' boron-lined tubes and Symetrica's LiF/ZnS(Ag) scintillator, both of which were designed against the ^{3}He HLNCC-II standard.

II. Neutron Coincidence and Multiplicity Counting

Neutron coincidence and multiplicity counters are important tools in nuclear facilities safeguards. These counters are designed and optimized to exploit the properties and reaction products of nuclear fission for the characterization of particular nuclear material samples. To calculate the total mass of the sample, the isotopic composition is determined, typically by a high-resolution gamma-ray measurement, and the effective mass can be determined from time-correlated neutron counting data.

The simultaneous emission of multiple neutrons from fission in SNM allows for coincidence detections from a single originating event. The fission timescale is less than a picosecond, typically releasing between one and three prompt neutrons. The fission chain propagation occurs over tens of nanoseconds, and the detection timescale of relevant thermal well detectors is on the order of tens of microseconds. However, background and (α, n) reactions also contribute to the total neutron counts. Neutrons from the same fission event are detected close to each other in time, whereas neutrons from nonfission processes are randomly distributed in time.

Using time-correlation methods allow these counters to discriminate against this background and distinguish between events. Singles (or totals), doubles (or reals), and triples count rates can be determined based on time-correlation of the measured pulse train. The singles count rate corresponds to the total number of measured neutrons. The doubles count rate corresponds to two neutron events measured within a specified time gate, and the triples count rate corresponds to three neutron events within that gate. The use of triples data is the characteristic of multiplicity counters, thereby allowing one to solve for three nuclear material sample unknowns, whereas coincidence counters use only singles and doubles data, allowing for the solution of two unknowns. Therefore, neutron coincidence and multiplicity counters must possess high enough efficiencies to detect correlated events with precision and reasonable dead time to maintain similar coincidence gate fractions to existing ^{3}He detectors [29].

Characteristics such as neutron die-away time, efficiency, and figure of merit (FOM) are used to quantify the performance of a counter. Neutron die-away time is a measure of the time it takes for a neutron emitted inside the detector cavity to thermalize and be detected. A short neutron die-away time is desired to improve measurement precision through a lower accidental count subtraction for a given counting time, but it is not always achievable based on the counter design. The efficiency is the probability of the counter detecting a neutron emitted by a nuclear material sample. The FOM is commonly the principal value reported when evaluating the response of

IEEE Proof

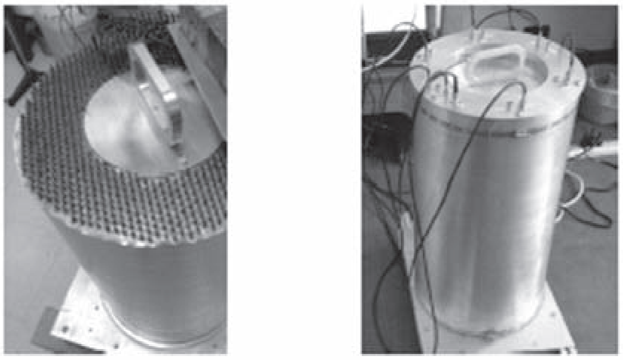

Fig. 1. BCS HLNCC-II model built by PTI. Straws uniformly dispersed within the cylindrical HDPE body with central sample cavity (left). Sealed BCS HLNCC with six outputs (right) [3].

these new proposed technologies; it is simply the efficiency over the square root of the neutron die-away time. The FOM is proportional to the neutron coincidence assay error, assuming all other factors such as sample type and count time stay constant. The goal of each of these alternative system designs is to match, or improve, the FOM of preexisting ^{3}He-based systems.

III. Boron-Coated Straw Detector

The BCS-based counter has been built by PTI as a direct replacement to the HLNCC-II [30], [31]. The performance of these straws in homeland security applications has already been shown and reported [32], [33], and currently, the development and characterization for thermal well detector designs is underway. As discussed in [30]–[33], BCS systems have the absolute detection efficiency desired, they possess sufficient gamma discrimination with set energy thresholds, and they maintain their neutron detection rate in relevant operational temperature ranges.

The BCS-based HLNCC-II is composed of 804 ^{10}B straws, each 4.4 mm in diameter, allowing for a tight packing within the geometry as a method to help improve detection efficiency. $^{10}B_4C$ at 96% enrichment is sputtered along the inside of an aluminum or copper straw with a thickness of approximately 2 μm and filled with a mixture of CO_2 (10%) and Ar (90%) at 1 atm. The dimensions of the ^{3}He HLNCC-II are preserved, although there is an increase in mass of 6 kg; it consists of a cylindrical high-density polyethylene (HDPE) body with a diameter of 34 cm and a height of 68.2 cm (Fig. 1). The sample cavity is 17 cm in diameter and 41 cm in height and is sealed with top and bottom end plugs made of HDPE and aluminum. There are six detector banks, of 134 tubes each, connected together and processed by six amplifiers. The 804 straws are uniformly dispersed within the moderator for the thermalization of neutrons.

The signal from the BCS system is passed through an external summation box consisting of six inputs, a shaping and amplifying circuit, and one signal output. Within this amplifying circuit, each of the pulses from the six detector banks can pass through logic gates in a field-programmable gate array module, providing pulse shaping and amplification to produce the correct form for the signal trigger. This signal can then be read out with standard shift register electronics.

The JSR-12 Neutron Coincidence Analyzer, designed by LANL and built by Canberra Industries Inc., counts and records pulses from neutron events and their time-correlations for coincidence and multiplicity counting. The BCS detector signal output can be measured as either a transistor–transistor logic (TTL) pulse input transmitted by a coaxial cable, or a differential pair of signals transmitted by a twisted pair cable; the JSR-12 can read the TTL pulses. The JSR-12 has a port which outputs a user-selected HV to power the detector. A coaxial cable can also be connected to the +5 V output port to provide power to the preamplifier or discriminator boards of the BCS detector.

The JSR-12 is compatible with the LANL neutron coincidence counting (INCC) computer program [34], used by the IAEA, through a universal serial bus connection. A graphical user interface enables communication to the shift register and coincidence counter. Within this software, parameters such as HV, gate width, dead time, and predelay can be selected and adjusted. The number of data acquisition runs and their duration can be chosen. A read out summary of these cycles shows the totals and reals with uncertainty for the signal input, and totals for the two auxiliary scalar inputs, in addition to other relevant parameters. For this benchmark exercise, each of the six detector bank signals was passed through the PTI summation box providing a total detector output. This total signal was then measured as a TTL pulse input to the JSR-12 using a coaxial cable. The BCS detector was powered to 850 V through the shift register. At the time of measurement, the +5 V output from the JSR-12 was not functioning properly with the BCS detector, so an external power supply was used directly connected to the +5 V input on the BCS detector. The results were read out in the INCC program on a personal computer.

IV. Characterization Measurements

The previously listed instruments (see Section I) were assessed by their respective developers at the Performance Laboratory for Safeguards in terms of high-voltage characteristic in the presence of ^{252}Cf and ^{137}Cs sources to investigate gamma discrimination, neutron detection efficiency, and die-away time using a characterized ^{252}Cf source using a common approach. A side-by-side comparison of each system's response to a range of SNM samples with statistical uncertainty in comparison to the respective ^{3}He standard model was also conducted.

Background rates varied based on what sources were present in the room at the time of the measurement, due to various detectors being tested simultaneously in close proximity. However, the singles (or totals) background rates were always much less than the count rates of the item being measured, and the background doubles (or reals) count rate was almost negligible. The background was measured prior to each data acquisition to ensure proper corrections would be applied.

Analyzing data previously acquired by Lacy *et al.* at PTI, using sealed ^{252}Cf sources and a JSR-12, the doubles count AQ:2

IEEE Proof

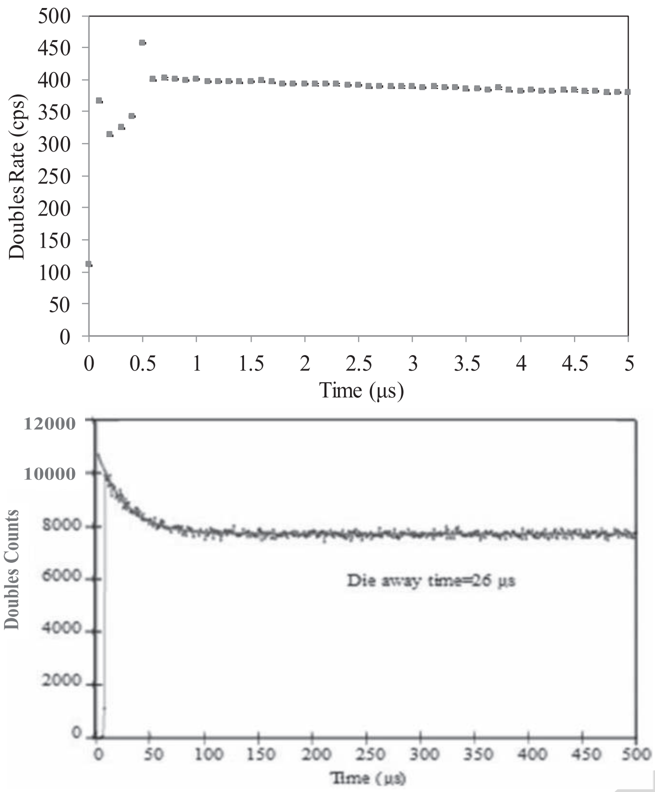

Fig. 2. Close-up view of a Rossi Alpha distribution used to determine predelay and gate width selection (top). Full Rossi Alpha distribution and fit with an exponential decay and linear accidental term to extract the die-away time (bottom).

rates were calculated for varying combinations of predelay lengths and gate widths. From these rates, the optimal values for the predelay and gate width were selected, 2 and 48 μs, respectively. Deviating slightly from the predelay and gate width values of the standard HLNCC-II, from 3 to 2 μs and from 32 to 48 μs, respectively, allows a large enough time window to detect correlated neutrons while limiting the number of accidental counts, and it prevents omitting a large fraction of counts at the beginning of the collection. Later, a Rossi Alpha distribution produced for the BCS counter using a 16 000 n/s ^{252}Cf source with list mode data acquisition was performed to investigate the predelay selection. The distribution supported this selection, revealing structured behavior between 0 and 0.5 μs, but a stable response after 0.6 μs (Fig. 2).

The die-away time τ was also obtained from the JSR-12-recorded data. Fitting an exponential decay plus a linear accidental term to the reals, through chi-squared analysis and minimizing the sum of squared errors, provided a die-away time of 26 μs. This die-away time determined by PTI has since been verified at the Oak Ridge National Laboratory.

To begin the benchmark measurements, a 17 500 n/s ^{252}Cf source was used to measure the HV characteristic to verify the operating voltage of the system. During this time, the neighboring test station in the room was supplied the strongest ^{252}Cf source available, thereby increasing the totals background count rate at the BCS counter station to an average of 10 Hz. It is important to note that the counting

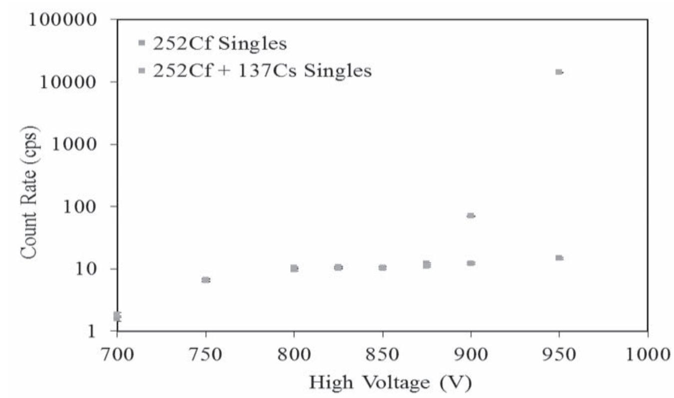

Fig. 3. High-voltage characteristic of the singles count rate produced using solely a ^{252}Cf source, and another in the presence of both a background ^{252}Cf and a ^{137}Cs source. Gamma breakdown begins after 875 V.

curve generated using a BCS detector does not have an HV plateau, unlike a ^{3}He detector, since its differential pulse height spectrum extends to zero with no physical gamma-to-neutron signal gap. Instead, this region has a slight increasing linear trend. Because of this, an operating voltage must be selected based on optimizing efficiency and gamma discrimination, and not the standard ^{3}He method of approximately 40 V above the knee.

A 10 mCi ^{137}Cs source was then introduced within the BCS, alongside the ^{252}Cf at the neighboring station, to test the response of the counter in a high gamma field (Fig. 3). The influence on count rate from the incident gamma rays is not evident until after 875 V. Below this point, the count rate is in agreement with the count rate from the ^{252}Cf source alone, proving the BCS capability of discrimination between neutron and gamma events. Throughout this region, the measured count rate follows this slight increasing trend, so a selection of an operating voltage throughout this regime will suffice. After 875 V, the detector signal is dominated by gamma counts. Based on this information, the detector was run at 850 V for all future measurements. Lacy *et al.* [30] have previously determined the gamma rejection ratio of their BCS in the range of HLNCC-II-relevant gamma exposure fields with selected energy cutoff thresholds [30]. For various straw geometry prototypes, the gamma discrimination ranges from 10^6 to 10^8.

Efficiency and dead-time measurements were taken using four ^{252}Cf sources of varying strengths. The certified source strengths are listed in Table I. It should be noted that not all sources have a National Physical Laboratory (NPL) certificate. Without proper characterization and uncertainty in the source strength, the accuracy of any future measurements will be affected.

The measured count rate of each source was background and dead-time corrected (DTC) using the well accepted DTC approach [35], [36]. The correction factors are

$$\mathrm{CF}_D = e^{\delta_R \cdot S_m} = e^{(a+b\cdot S_m)\cdot S_m} \quad (1)$$

$$\mathrm{CF}_S = e^{\delta_T \cdot S_m} = e^{\frac{1}{4}(a+b\cdot S_m)\cdot S_m} = \mathrm{CF}_D^{1/4} \quad (2)$$

where S_m is the measured singles (totals) rate and a and b are dead-time parameters which are empirically determined

IEEE Proof

TABLE I

^{252}Cf SOURCE STRENGTHS

Source	Intensity (n/s)	Relative Standard Deviation (%)	NPL Certificate
5549NC	17500 ± 200	1.14	No
5987NC	7050 ± 70	0.993	Yes
6005NC	513 ± 20	3.90	Yes
*H9-716	171354.5 ± 1782.1	1.04	Yes

* Intensity calculated on 10/14/2014. Previous records of count rate provided by National Institute of Standards and Technology (NIST). All other intensities given on 10/13/2014. Measurements taken on 10/13/2014.

TABLE II

DEAD-TIME AND BACKGROUND CORRECTED ^{252}Cf COUNT RATES

Source	Totals (cps)	± (cps)	Reals (cps)	± (cps)	Reals/Totals	± (cps)
5549NC	2689.2	2.5	425.3	1.9	0.15815	0.00050
5987NC	955.7	1.5	155.60	0.87	0.16280	0.00095
6005NC	72.59	0.43	11.58	0.19	0.1594	0.0028
H9-716	22973.3	7.5	3779.	13	0.16450	0.00058

TABLE III

EFFICIENCY MEASUREMENTS USING ^{252}Cf SOURCES

Source	Efficiency (%)	± (%)	Relative Standard Deviation (%)
5549NC	15.37	0.18	1.1
5987NC	13.56	0.14	1.0
6005NC	14.15	0.56	3.9
*H9-716	13.41	0.14	1.0
Mean	14.12		

*Extra 0.03% uncertainty from 10% deviation from unity on the totals DTC.

TABLE IV

EFFICIENCY MEASUREMENTS AS A FUNCTION OF INCIDENT NEUTRON ENERGY

Source	Efficiency (%)	± (%)	Relative Standard Deviation (%)	<E> (MeV)	± (%)
^{252}Cf	13.93	0.14	1	2.12	0.05
AmLi	20.06	0.36	1.8	0.53	0.05
AmBe	9.299	0.088	0.95	4.2	0.1

for a specific detection system. The free parameters a and b are empirically determined by applying a quadratic fit to doubles count rate data as a function of increasing singles rate. To then calculate the DTC rates, the measured count rates are multiplied by the correction factor

$$D_{\text{DTC}} = \text{CF}_D \cdot D_m \tag{3}$$

$$S_{\text{DTC}} = \text{CF}_S \cdot S_m. \tag{4}$$

After applying the dead-time and background rate corrections, the reals-to-totals (R/T) ratio was taken. The ratio was analyzed through another chi-squared analysis. The sum of squared errors of the deviation between the DTC R/T and the variable R/T parameter over the uncertainty in the DTC R/T was minimized with respect to a and the R/T parameter. Through this analysis, the sources provided were discovered to be too weak to produce meaningful dead-time parameters. Instead, parameters from previous data acquisition at PTI were used, 0.55 and 0 μs for a and b, respectively. The R/T parameter used for ^{252}Cf was 0.1612. These values were obtained through similar analysis using three National Institute of Standards and Technology certified sources of measured strengths (746.64 ± 0.86), (15999.10 ± 6.46), and (377338.40 ± 30.57) Hz.

These dead-time parameters were used with (1)–(4) to find the DTC rates for totals and reals which were then background corrected. R/T is also reported in Table II for a comparison between sources.

The detection efficiencies of these ^{252}Cf sources at 850 V were then determined. Data were taken with each of the sources placed in the center of the well, with 0.2% positional uncertainty, for 20 cycles of 30 s each. Each acquisition was repeated and a corresponding background run was taken. Using the source strength and the fully corrected total count rate, the efficiency was calculated. Table III shows the results. The difference in calculated efficiency values using the four sources is larger than anticipated, influencing the mean measured efficiency. Because each of the sources had varying measurement uncertainties, each source was given differing weights toward a summed efficiency of the detector. This weighted mean efficiency of 13.93% is used in our calculations. When selecting a single source for the representation of efficiency, 5987NC was selected as the most reliable due to the low relative standard deviation in combination with having the corresponding NPL certificate.

Two other sources, identified as ANHP-N252, an AmLi source having (113400 ± 2000) n/s and NK4442, an AmBe source having (21220 ± 200) n/s, were then used to test the efficiency as a function of incident neutron energy. The average neutron energy from the AmLi source is much lower than the ^{252}Cf, approximately 0.5 MeV in comparison to 2.13 MeV, and the AmBe source is much higher at 4.2 MeV. Twenty measurement cycles of 30 s each were run. As expected when using a random (rather than time-correlated) neutron AmLi source, the measured net reals, (2.2 ± 9.2) Hz, was consistent with zero. The net reals with the AmBe source also behaved as expected, showing a small increase in neutron count rate, (8.93 ± 0.81) Hz, due to the ^{9}Be (n, $2n$) contribution. The efficiencies for these sources are compared with the weighted efficiency of the ^{252}Cf sources in Table IV.

The measured efficiencies are plotted in Fig. 4. Based on these values alone, the efficiency for ^{240}Pu with average energy of 1.96 MeV may be estimated to be approximately 14.44%.

After the successful performance of the BCS in each of these tasks was verified, data were compared between systems. A measurement was conducted with the ^{252}Cf source 5987NC placed within the well of several HLNCC-type prototypes: the benchmark ^{3}He HLNCC-II, GE Reuter-Stokes ^{10}B-lined tubes, ^{6}Li/ZnS-based HLNCC, and the BCS. Only the BCS detector was able to match and exceed the ^{3}He HLNCC-II equivalent system as is (Table V); each respective supplier has since returned to improve the response of their model.

IEEE Proof

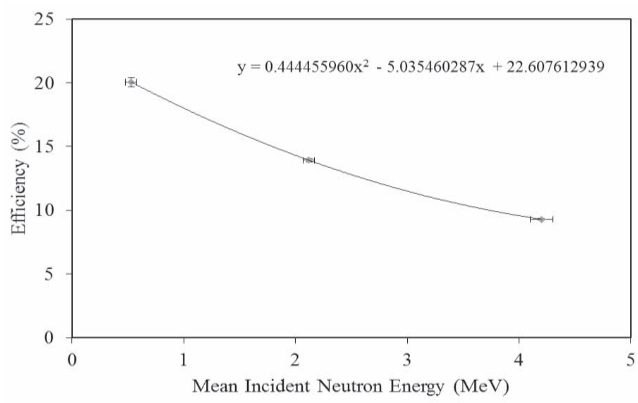

Fig. 4. Efficiency measurements for various neutron sources. A quadratic fit was applied to these data to estimate the efficiency of a ^{240}Pu source.

TABLE V
COMPARISON OF HLNCC-BASED PROTOTYPES [3]

Safeguards Parameters	^{3}He-based HLNCC	GE Reuter Stokes ^{10}B-lined tubes	^{6}Li/ZnS based HLNCC*	BCS-based HLNCC
Efficiency, ε (%)	16.50	10.20	8.90	13.56
Die-away time, τ (μs)	43.30	65.40	55.90	26.00
FOM (ε/√τ)	2.51	1.26	1.19	2.66

*Results for ^{6}Li/ZnS based HLNCC represent values for partial system (eight contrary to 24 blades).

The lower die-away time measured for the BCS is attributed to the near-uniform dispersion of the ^{10}B absorber within the HDPE neutron moderator. Despite a lower efficiency, the FOM of the BCS is better than that of the ^{3}He HLNCC-II because of the shorter die-away time advantage, meeting the requirements set for an alternative design. Although this value is dependent on the discrimination established for the 10 mCi ^{137}Cs source, this FOM is valid for routine contact-handling materials, covering a broad range of samples measured by counters such as the HLNCC-II. Some samples designated to be measured within the HLNCC-II do exceed this gamma rate, however. Further measurements would be needed to establish the gamma dose limit and its effect on the FOM comparison to the HLNCC-II in these higher dose scenarios.

V. NONDESTRUCTIVE ASSAY MEASUREMENTS

Additionally, several ^{240}Pu sources in varying compositions and geometries were then measured in the BCS counter (Table VI). The effective weight percent w_{eff} was calculated for each of the samples based on given isotopics and available nuclear data. The weight percents were calculated for the first day of measurement and then used for all successive measurements, introducing a negligible uncertainty due to further decay.

The weight percents were independently recalculated by another member of the team with similar results, yet the values were not in perfect agreement. Discrepancies in the decay corrected values can stem from different choices in sources of nuclear data, specifically the influence of the uncertainty (±0.1 year) between quoted values of the ^{241}Pu half-life. The ingrowth of ^{241}Am has a very large uncertainty as it is a function of the decay of Pu. Propagation of these errors through final calculations was investigated, and the leading uncertainty was included.

TABLE VI
^{240}Pu ISOTOPICS

Source	Form	Geometry	^{240}Pu Wt Percent (%)
CBNM Pu 93	PuO_2	40 mm × 21 mm can	6.401
CBNM Pu 61a	PuO_2	40 mm × 21 mm can	36.75
CBNM Pu 61b	PuO_2	40 mm × 21 mm can	36.75
PuGa #32	Alloy	0.6 mm × 36.5 mm disk	5.978
ENEA-01	MOX	~130 mm × 95 mm can	32.66

The measured count rates are related to the properties of the sample, the parameters of the detection system, and basic nuclear data through point model equations, based on the Ensslin–Krick approach [37], to quantify the mass of a fissioning sample.

The dead-time and background corrected totals and reals count rate can be found by

$$T = m_{\mathrm{eff}} g \varepsilon \nu_1 M (1+\alpha) \tag{5}$$

$$R = m_{\mathrm{eff}} g \varepsilon^2 f \frac{\nu_2}{2} M^2 [1 + (1+\alpha)(M-1)K] \tag{6}$$

where m_{eff} is the effective mass of ^{240}Pu in the sample to produce the measured rates, g is the specific spontaneous fission rate for ^{240}Pu, ε is the detector efficiency, f is the reals gate fraction, M is the leakage self-multiplication, α is the ratio between the number of random neutrons produced through (α, n) reactions and spontaneous fission neutrons, and ν_i is the ith factorial moment of the prompt multiplicity distribution of the source of fission neutrons. The contribution from both induced (I) and spontaneous (S) fission is contained in

$$K = \frac{\nu_{S1}}{(\nu_{I1} - 1)} \cdot \frac{\nu_{I2}}{\nu_{S2}} \tag{7}$$

where the factorial moments are based on basic nuclear data. In contrast to the factorial moments, the alpha value, or (8), is expected to vary from item to item depending on its composition

$$\alpha = \frac{(\alpha, n)_{\mathrm{rate}}}{(SF, n)_{\mathrm{rate}}}. \tag{8}$$

The dependence of K on the incident energy spectrum between (α, n) reactions inducing fission and (SF, n) events is ignored, and K is treated as a constant. It is therefore assumed that the neutrons from both contributors are detected at the same efficiency. In reality, there is approximately 1%–2% spread in efficiency, introducing more uncertainty into the calculation. The quantity α is treated as independent of K and other terms due to the dominating uncertainty in the chemical form such as impurity content and microstructure changing the contributors of the constituents, overshadowing any correlation between these two parameters. The $(\alpha, n)_{\mathrm{rate}}$ can be estimated from nuclear data with known coefficients for the $(\alpha, , n)_{\mathrm{rate}}$

IEEE Proof

in oxygen per gram, assuming stoichiometry, but impurities introduce deviations from these values.

The effective mass of the fissioning ^{240}Pu is found by

$$m_{\text{eff}} = \frac{R_c}{a} \tag{9}$$

where a is an estimated parameter based on the fact that the calibration is based off of ^{252}Cf. The multiplication corrected reals rate, R_c, is represented by

$$R_c = \frac{\rho_0}{a} \cdot \frac{T}{M(1+\alpha)} = b \cdot \frac{T}{M(1+\alpha)} \tag{10}$$

with R/T for nonmultiplying ^{240}Pu metal ρ_0 as an empirical parameter used to compensate for point model violations. This is represented by

$$\rho_0 = \frac{\varepsilon f \frac{\nu_2}{2}}{\nu_1} \tag{11}$$

for the usual point model used to interpret neutron coincidence counting data and

$$\rho_0 = \frac{\frac{R}{T}(1+\alpha)}{M[1+(1+\alpha)(M-1)K]} \tag{12}$$

for a pure reference oxide item. Although ρ_0 can be calculated through basic nuclear parameters, it is assumed in this case that ρ_0 may be treated as independently known; therefore, these two equations are equal in this context. The quantity b is then a constant of proportionality for direct scaling used with the adjusted totals. It is obtained through calibration with similar items.

Typically for assay benchmarks, one is given a minimum of three samples of Pu of similar composition yet marginally different sizes to measure. Values from these known samples can be extrapolated, generating coefficients for calibration, to apply to unknown samples of similar sizes. However, this was not the case; because of the lack of similar sources, given both metallic and oxide sources, an accurate calibration is incredibly difficult and leads to values which violate the point model.

The leakage self-multiplication is represented by

$$M = \frac{[K(1+\alpha)-1] + \sqrt{\frac{[K(1+\alpha)-1]^2 + 4K(1+\alpha)^2 \frac{R}{T}}{\rho_0}}}{2K(1+\alpha)}. \tag{13}$$

Sometimes due to violations of the point model such as the fact that (α, n), (SF, n), and physically small items will have different detection efficiencies, but are assumed to have the same, M can be less than unity. This value must be clamped at 1 for these cases to ensure the result makes physical sense, but this then alters the linearity of the calculations. With a final substitution, the multiplication corrected reals rate can be found.

These equations were used with the nuclear data and calibration parameters (Table VII) to calculate the ^{240}Pu m_{eff}, the leakage self-multiplication, the total sample mass, and the deviation of the calculated mass from the declared mass (Table VIII). The reals gate utilization factor was assumed to be the same for ^{252}Cf and ^{240}Pu, 0.779, from the previously measured data. The uncertainty of each term was calculated at $\pm 1\sigma$ through brute force numerical methods to produce a final combined uncertainty. Considering all the sources of uncertainty introduced throughout this calibration and assay, a deviation of approximately 2% across the diversity of these samples is satisfactory.

TABLE VII
CALIBRATION PARAMETERS

Parameter	Value	±
K	2.175	0.010
ρ_0	0.1043	0.0023
a	14.60	0.29
b	0.007142	0.000071

TABLE VIII
^{240}Pu ASSAY RESULTS

Source	Declared mass (g)	M	Calculated mass (g)	± (g)	Deviation (%)
CBNM Pu 93	5.825	1.0103	5.98	0.11	2.66
CBNM Pu 61a	5.528	1.0163	5.40	0.11	-2.32
CBNM Pu 61b	5.528	1.0160	5.41	0.11	-2.13
PuGa #32	9.389	*1.000	9.45	0.22	0.65
ENEA-01	163.845	*1.000	161.60	3.35	-1.37

*Initial results were M <1. Multiplication was clamped at M = 1.

VI. CONCLUSION

The FOM of a BCS-based well counter designed as a ^{3}He replacement has been found to be 2.66 under specified conditions regarding gamma sample rates. Under the same conditions, the FOM of the ^{3}He-based HLNCC-II model was found to be 2.51. Despite the BCS system's lower efficiency, its shorter die-away time improves the FOM such that it is comparable with the ^{3}He-based HLNCC-II. Although the FOM is not the only criteria for successful deployment, it is a minimum requirement.

Additionally, the system met the requirements presented at the described ^{3}He alternatives for International Safeguards Workshop. In this paper, the optimal operating voltage, predelay and gate width timing values, and dead-time parameters were determined using said sources. Gram quantity Pu sample assay results for the BCS-based coincidence counter are also reported.

The performance at higher gamma rates also needs further exploration, in order to understand how well it can be expected to perform in measurement of kilogram quantities of mixed oxide materials. The use of a list mode data acquisition system could also be explored.

ACKNOWLEDGMENT

AQ:3

The United States Government retains and the publisher, by accepting the article for publication, acknowledges that the United States Government retains a nonexclusive, paid-up, irrevocable, worldwide license to publish or reproduce the published form of this manuscript, or allow others to do so, for United States Government purposes. The Department of Energy will provide public access to these results of federally

IEEE Proof

sponsored research in accordance with the DOE Public Access Plan (http://energy.gov/downloads/doe-public-access-plan).

REFERENCES

[1] R. T. Kouzes, "The ^{3}He supply problem," Pacific Northwest Nat. Lab., Richland, WA, USA, Tech. Rep., 2009. AQ:4

[2] R. T. Kouzes, A. T. Lintereur, and E. R. Siciliano, "Progress in alternative neutron detection to address the helium-3 shortage," *Nucl. Instrum. Methods Phys. Res. A, Accel. Spectrom. Detect. Assoc. Equip.*, vol. 784, pp. 172–175, Jun. 2015.

[3] D. Henzlova *et al.*, "Current status of helium-3 alternative technologies for nuclear safeguards," Los Alamos Nat. Lab., Los Alamos, NM, USA, Tech. Rep., 2015.

[4] R. Van Ginhoven, R. Kouzes, and D. Stephens, "Alternative neutron detector technologies for homeland security," Pacific Northwest Nat. Lab., Richland, WA, USA, Tech. Rep. PNNL-18471, 2009. AQ:5

[5] M. Bliss *et al.*, "Glass-fiber-based neutron detectors for high- and low-flux environments," *Proc. SPIE*, vol. 2551, pp. 108–117, 1995. AQ:6

[6] R. Seymour, B. Richardson, M. Morichi, M. Bliss, R. Craig, and D. Sunberg, "Scintillating-glass-fiber neutron sensors, their application and performance for plutonium detection and monitoring," *J. Radioanal. Nucl. Chem.*, vol. 243, no. 2, pp. 387–388, 2000.

[7] J. H. Ely, L. E. Erikson, R. T. Kouzes, A. T. Lintereur, and E. R. Siciliano, "Lithium loaded glass fiber neutron detector tests," Pacific Northwest Nat. Lab., Richland, WA, USA, Techn. Rep. PNNL-18988, 2009.

[8] H. O. Menlove, D. Henzlova, L. G. Evans, M. T. Swinhoe, and J. B. Marlow, "^{3}He replacement for nuclear safeguards applications—An integrated test program to compare alternative neutron detectors," *ESARDA Bull.*, vol. 46, pp. 12–19, May 2011.

[9] S. M. Robinson, S. Stave, A. Lintereur, E. Siciliano, R. Kouzes, and M. Bliss, "Neutron pileup algorithms for multiplicity counters," *Nucl. Instrum. Methods Phys. Res. A, Accel. Spectrom. Detect. Assoc. Equip.*, vol. 784, pp. 293–297, Jun. 2015.

[10] M. Browne *et al.*, "Prototype neutron-capture counter for fast-coincidence assay of plutonium in residues," to be published. AQ:7

[11] K. A. Nelson *et al.*, "Investigation of a lithium foil multi-wire proportional counter for potential ^{3}He replacement," *Nucl. Instrum. Methods Phys. Res. A, Accel. Spectrom. Detect. Assoc. Equip.*, vol. 669, pp. 79–84, Mar. 2012.

[12] K. Wilhelm, J. Nattress, and I. Jovanovic, "Development and operation of a ^{6}LiF:ZnS(Ag)—Scintillating plastic capture-gated detector," *Nucl. Instrum. Methods Phys. Res. A, Accel. Spectrom. Detect. Assoc. Equip.*, vol. 842, pp. 54–61, Jan. 2017.

[13] J. H. Ely, E. R. Siciliano, M. T. Swinhoe, and A. T. Lintereur, "Modeling and simulation optimization and feasibility studies for the neutron detection without helium-3 project," Pacific Northwest Nat. Lab., Richland, WA, USA, Tech. Rep., 2011.

[14] J. H. Ely, M. Bliss, R. T. Kouzes, and A. T. Lintereur, "Final technical report for the neutron detection without helium-3 project," Pacific Northwest Nat. Lab., Richland, WA, USA, Tech. Rep., 2013.

[15] S. Stave *et al.*, "LiF/ZnS neutron multiplicity counter," *Nucl. Instrum. Methods Phys. Res. A, Accel. Spectrom. Detect. Assoc. Equip.*, vol. 784, pp. 208–212, Jun. 2015.

[16] M. Schear, D. Ramsden, G. Dermody, H. Tagziria, P. Peerani, and B. Pedersen, "Monte Carlo modelling and experimental evaluation of a ^{6}LiF:ZnS (Ag) test module for use in nuclear safeguards neutron coincidence counting applications," Tech. Rep., 2015. AQ:8

[17] A. Lavietes *et al.*, "Liquid scintillator-based neutron detector development," in *Proc. IEEE Nucl. Sci. Symp. Med. Imag. Conf. (NSS/MIC)*, Oct./Nov. 2012, pp. 230–244.

[18] M. D. Aspinall, M. J. Joyce, F. D. Cave, R. Plenteda, and A. Tomanin, "Automated response matching for organic scintillation detector arrays," *Nucl. Instrum. Methods Phys. Res. A, Accel. Spectrom. Detect. Assoc. Equip.*, vol. 861, pp. 46–54, Jul. 2017. AQ:9

[19] K. C. Frame, W. A. Clay, W. H. Geist, J. P. Lestone, A. P. Belian, and K. D. Ianakiev, "Neutron and gamma pulse shape discrimination in a liquid scintillator counter for neutron multiplicity measurements of enriched uranium," Los Alamos Nat. Lab., Los Alamos, NM, USA, Tech. Rep., 2004.

[20] M. J. Marcath, T. H. Shin, S. D. Clarke, P. Peerani, and S. A. Pozzi, "Neutron angular distribution in plutonium-240 spontaneous fission," *Nucl. Instrum. Methods Phys. Res. A, Accel. Spectrom. Detect. Assoc. Equip.*, vol. 830, pp. 163–169, Sep. 2016.

[21] A. Di Fulvio *et al.*, "Fast multiplicity counter featuring stilbene detectors for special nuclear material assay," in *Proc. IEEE Nucl. Sci. Symp. Med. Imag. Conf. (NSS/MIC)*, Oct./Nov. 2015, pp. 1–4.

[22] A. Di Fulvio *et al.*, "Passive assay of plutonium metal plates using a fast-neutron multiplicity counter," *Nucl. Instrum. Methods Phys. Res. A, Accel. Spectrom. Detect. Assoc. Equip.*, vol. 855, pp. 92–101, May 2017.

[23] D. Henzlova, H. O. Menlove, and J. B. Marlow, "Design and performance of a ^{3}He-free coincidence counter based on parallel plate boron-lined proportional technology," *Nucl. Instrum. Methods Phys. Res. A, Accel. Spectrom. Detect. Assoc. Equip.*, vol. 788, pp. 188–193, Jul. 2015.

[24] D. Henzlova and H. O. Menlove, "High-dose neutron detector development," Los Alamos Nat. Lab., Los Alamos, NM, USA, Tech. Rep., 2016.

[25] H. O. Menlove and D. Henzlova, "Improvements in boron plate coating technology for higher efficiency neutron detection and coincidence counting error reduction," Los Alamos Nat. Lab., Los Alamos, NM, USA, Tech. Rep., 2016.

[26] R. T. Kouzes, J. H. Ely, A. T. Lintereur, and E. R. Siciliano, "Boron-10 ABUNCL prototype models and initial active testing," Pacific Northwest Nat. Lab., Richland, WA, USA, Tech. Rep. PNNL-22424, 2013.

[27] R. T. Kouzes, J. H. Ely, A. T. Lintereur, and E. R. Siciliano, "Boron-10 based neutron coincidence counter for safeguards," *IEEE Trans. Nucl. Sci.*, vol. 61, no. 5, pp. 2608–2618, Oct. 2014.

[28] R. D. McElroy and S. Croft, "Application of ^{10}B-lined proportional counters to traditional neutron counting applications in international safeguards," Oak Ridge Nat. Lab., Oak Ridge, TN, USA, Tech. Rep., 2014.

[29] L. G. Evans *et al.*, "Nuclear safeguards ^{3}He replacement requirements," *J. Nucl. Mater. Manage.*, vol. 40, p. 88, 2012. AQ:10

[30] J. L. Lacy, A. Athanasiades, C. S. Martin, L. Sun, and G. J. Vazquez-Flores, "Design and performance of high-efficiency counters based on boron-lined straw detectors," in *Proc. 53rd Annu. Meet. Inst. Nucl. Mater. Manage. (INMM)*, 2012. AQ:11

[31] J. L. Lacy, A. Athanasiades, L. Sun, C. S. Martin, G. J. Vazquez-Flores, and S. Mukhopadhyay, "Performance of a straw-based portable neutron coincidence/multiplicity counter," in *Proc. IEEE Nucl. Sci. Symp. Med. Imag. Conf. (NSS/MIC)*, Oct. 2011, pp. 529–532.

[32] J. L. Lacy, A. Athanasiades, C. S. Martin, L. Sun, and G. L. Vazquez-Flores, "The evolution of neutron straw detector applications in homeland security," *IEEE Trans. Nucl. Sci.*, vol. 60, no. 2, pp. 1140–1146, Apr. 2013.

[33] J. L. Lacy, A. Athanasiades, C. S. Martin, L. Sun, G. J. Vazquez-Flores, and T. D. Lyons, "Boron-coated straw detectors: A novel approach for helium-3 neutron detector replacement," in *Proc. IEEE Nucl. Sci. Symp. Conf. Rec. (NSS/MIC)*, Oct./Nov. 2010, pp. 3971–3975.

[34] B. Harker, M. Krick, W. Geist, and J. Longo, "INCC software users manual," Los Alamos Nat. Lab., Los Alamos, NM, USA, Tech. Rep. LA-UR-99-1291, Jul. 1998. AQ:12

[35] M. S. Krick and H. O. Menlove, "High-level neutron coincidence counter (HLNCC): Users' manual," Los Alamos Sci. Lab., Los Alamos, NM, USA, Tech. Rep. LA-7779-M, Jun. 1979.

[36] S. Croft, L. G. Evans, M. T. Swinhoe, D. K. Hauck, and P. A. Santi, "Testing an alternative singles rate dead time correction algorithm for use in neutron multiplicity analysis," in *Proc. 52nd Annu. INMM Meet.*, 2011. AQ:13

[37] N. Ensslin, J. E. Stewart, and J. Sapir, "Self-multiplication correction factors for neutron coincidence counting," *Nucl. Mater. Manage*, vol. 8, no. 2, pp. 60–73, 1979.

IEEE Proof